THE JOURNAL OF PHYSICAL CHEMISTRY C

Article

pubs.acs.org/JPCC

Temperature-Dependent Raman Study of $Gd@C_{82}$

Trisha Mondal,[†] Ajay Tripathi,[†] Jinying Zhang,[‡] Vasant Sathe,[§] T. Shripathi,[§] H. Shinohara,[∥] and Archana Tiwari*,[†]

[†]Department of Physics, School of Physical Sciences, Sikkim University, Gangtok, Sikkim 737102, India

[‡]Center of Nanomaterials for Renewable Energy, School of Electrical Engineering, Xian Jiaotong University, Xi'an, Shanxi Province 710054, China

[§]UGC-DAE CSR, Indore Centre, Khandwa Road, Indore 452001 (M.P.), India

[∥]Department of Chemistry and Institute for Advanced Research, Nagoya University, Nagoya 464-8602, Japan

ABSTRACT: We present a Raman spectroscopy investigation of the vibrational properties of a rare-earth endohedral metallofullerene, $Gd@C_{82}$, at low temperatures. While lowering the temperature, the Raman spectra show a blueshift in the Gd−C and C−C vibrational modes which are attributed to both anharmonic and thermal expansion contributions in the fullerene cage. The experimental data are compared with the theories of the shift and broadening of the phonon lines, and respective anharmonic and temperature coefficients are evaluated. In addition, the force constant of the Gd−C_{82} vibration is derived at various temperatures using a linear harmonic oscillator model. No change in the oxidation state of the ion is noted in the examined temperature range.

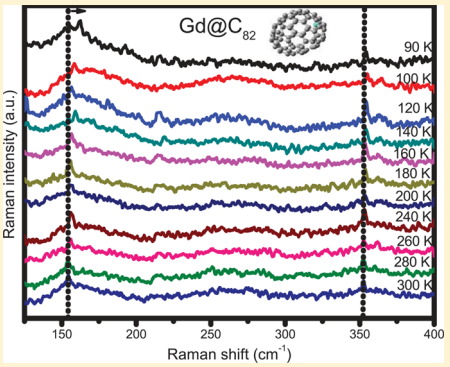

INTRODUCTION

Endohedral metallofullerenes (EMFs) with a metal ion encapsulated inside the cage exhibit interesting electrical, transport, optical, and magnetic properties.[1−3] The metal ions are positioned off-center within the cage wherefrom it transfers multiple electrons and exhibits strong metal−cage interactions.[1,4,5]

To date, two key vibrations are reported in detail in the Raman spectra of EMFs: (i) the cage internal vibrational modes and (ii) the metal ion−cage vibrational modes.[6] Large atomic masses of the metal ions in the cage often lead to low-frequency metal−cage Raman vibrations. The force constant of the metal−cage interaction depends on the electrostatic charge difference between the ion and cage. In various EMFs, such as La, Gd, Y, and Tm doped C_{82}, the force constants derived from Raman frequency of the metal−cage interactions are found to be different for the different ions. Under ambient conditions, the EMFs show a metal−cage stretching vibration below 200 cm^{-1}, whose frequencies shift by approximately +40 cm^{-1} when a triply charged metal ion (e.g., La^{3+} or Gd^{3+}) is incarcerated inside the cage instead of a doubly charged ion (e.g., Tm^{2+} or Eu^{2+}).[6−8] Any anharmonic interaction between the metal ion and cage may affect the phonon frequencies, their line widths, and the thermal conductivity of the fullerene. Similar studies have been performed on diamond crystals and other carbon nanomaterials at different temperatures where the changes in lattice parameters have been attributed to the variation in force constants, thermal expansion coefficients, and potential anharmonicity.[9−14]

Temperature-dependent Raman frequencies are also reported in $Sc_2@C_{84}$ and $C_2@Sc_2C_{84}$; in $Sc_2@C_{84}$, with a decrease in temperature, both downshifts and upshifts in the cage vibration frequencies are observed, whereas in $C_2@Sc_2C_{84}$ both moderate peak broadening and temperature-induced peak shift are reported.[15,16] In lanthanides (Ce, Yb) doped crystal, the valency of ion also reportedly varies with temperature.[17−19] However, variations in intramolecular interactions and the oxidation state of the doped ions in $M@C_{82}$ with temperatures have not been established to date.

In order to understand the metal−cage interactions in EMFs and their spectroscopic, magnetic, and structural properties, the knowledge of electron distribution in the fullerenes is important. In ambient conditions, Gd is found in its 3+ oxidation state, transferring three electrons to the C_{82} cage.[7,20] An addition of mechanical and thermal stress in fullerenes may enable manipulation of its electronic properties and electron transfer in the cage.

In this paper, we present temperature-dependent Raman studies of $Gd@C_{82}$. The Raman peaks due to Gd−cage and C−C vibration are observed for the temperature between 90 and 300 K. This study examines the incurred changes in the strength of metal−cage interaction and the charge transfer between the Gd ion and the cage at low temperatures.

Received: March 9, 2015
Revised: May 12, 2015
Published: May 20, 2015

DOI: 10.1021/acs.jpcc.5b02284
J. Phys. Chem. C 2015, 119, 12698−12702

MATERIALS AND METHODS

$Gd@C_{82}$ with a purity >98.5% was dissolved in carbon disulfide (CS_2). The dissolved sample was drop casted into thin film on the glass slides. Room-temperature Raman measurements were performed using a Renishaw inVia RM2000 spectrometer with 514.5 and 785 nm laser excitations and 30 mW power, whereas low-temperature Raman measurements were done using a LABRAM HR-800 spectrometer using 1800 L/mm grating and 632.8 nm excitation laser. The laser was operated so that 2 mW power was present at the sample in order to avoid sample heating. A 50× objective was used for both room- and low-temperature measurements, and the spectral resolution was better than 1 cm^{-1}. For low-temperature measurements the sample was mounted in a THMS-600 stage from Linkam, UK with a temperature stability of ±0.1 K from 90 to 300 K with a thermal step of 10 K. After background subtraction, Raman peak positions and widths were determined by fitting Lorenzian profiles.

RESULTS AND DISCUSSION

Room-temperature Raman spectra of $Gd@C_{82}$ thin films are shown in Figure 1 when excited with 514.5 and 785 nm laser excitations in the energy range between 100 and 600 cm^{-1}. Four distinct Raman peaks are observed near 155, 215, 398, and 470 cm^{-1}. The peak energies below 200 cm^{-1} are attributed to metal−cage vibrations, whereas higher-energy peaks are attributed to the cage internal vibrations.[6,7] Unlike previous reports, the presented spectra show smaller background and intense peaks in the energy range 100−600 cm^{-1}. This difference could be credited to less air exposure of $Gd@C_{82}$ in our study than the previous report.[6,7] Although room-temperature Raman studies have been extensively performed on the EMFs in the past, there is limited information on the intrafullerene interactions at low temperatures.

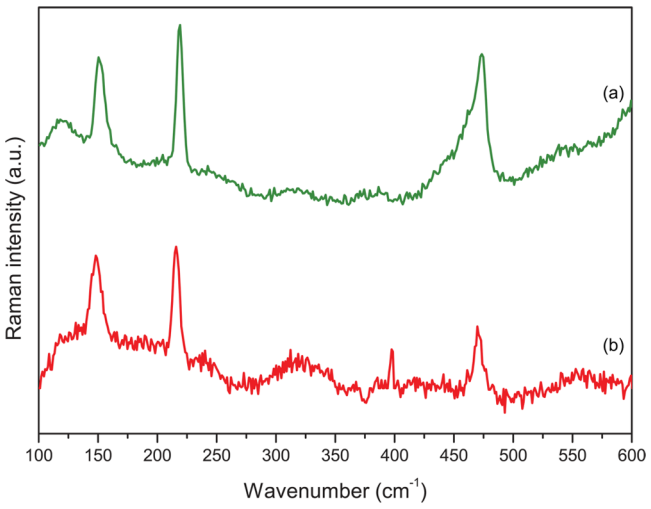

Figure 1. Room-temperature Raman spectra of $Gd@C_{82}$ obtained with excitation wavelengths (a) 514.5 nm and (b) 785 nm.

In order to understand the metal−cage and C−C interactions in the cage, the low-temperature Raman studies are performed on $Gd@C_{82}$ using 633 nm laser excitation. Raman spectra of $Gd@C_{82}$ in the temperature range 90−300 K are shown in Figure 2. Two peaks, at 155 and 352 cm^{-1}, are evident throughout in the low-temperature spectra. In addition to these, a weak peak at 215 cm^{-1} is also observed. Owing to their stronger intensities, we shall discuss the detailed changes in 155 and 352 cm^{-1} peaks with temperature in the following section.

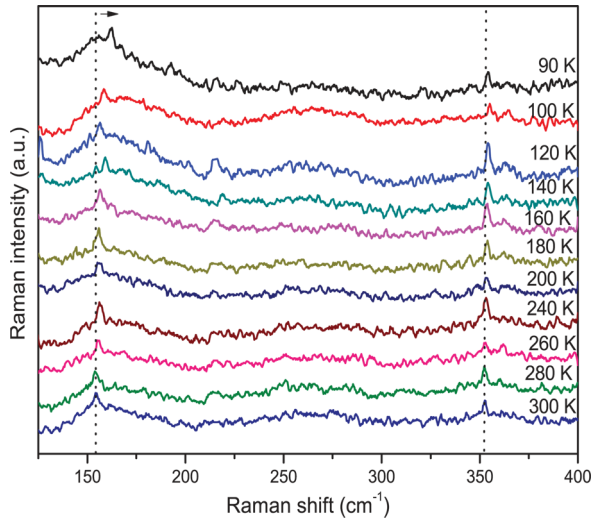

Figure 2. Temperature-dependent Raman spectra of $Gd@C_{82}$ obtained between 90 and 300 K with excitation wavelength 633 nm.

For the 155 and 352 cm^{-1} peak, the Raman peak positions are plotted versus the temperature and are shown in Figure 3. Upon lowering the temperature to 90 K, it is observed that both Raman peaks at 155 and 352 cm^{-1} are blue-shifted. For the 155 cm^{-1} peak, the shift in the peak position is evident only below 160 K. At 90 K, a shift of approximately +7.0(0.5) cm^{-1} is observed in the 155 cm^{-1} peak, whereas the peak at 352 cm^{-1} is shifted by +3(1) cm^{-1}. The measurements were repeated several times in order to verify the reproducibility of these small Raman shifts at low temperatures. Using a simple harmonic oscillator model for $Gd-C_{82}$, where the ion moves relative to the cage, the Raman vibrational frequency can be calculated[6,21]

$$\nu\ (\mathrm{cm}^{-1}) = 1302.1(k/\mu)^{1/2} \quad (1)$$

where k is the force constant (N cm^{-1}) between the ion and the cage and μ is the reduced mass of $Gd@C_{82}$ in a.m.u. From this equation, the force constants (k) are derived for the metal−cage vibrational mode (at 155 cm^{-1}) at different temperatures and are plotted in Figure 3(a) inset. At room temperature, k for $Gd-C_{82}$ is found to be 1.9 N cm^{-1}, whereas at 90 K, the k value increases to 2.1 N cm^{-1}. The change in force constants signifies variation in the nature and strength of the metal−cage interaction, which primarily depends on the oxidation state of the incarcerated ion and the charge transfer between the ion and cage.[22]

Magnetometry studies have been previously performed on $Gd@C_{82}$ in the temperature range 2−300 K.[23−26] The magnetization curves at different temperatures are well characterized by the Brillouin function B_J which depends on J, the total angular momentum, and g, the Lande g-factor. For a free rare-earth ion like Gd^{3+} with negligible spin−orbit coupling, J is a good quantum number.[24] Using the Brillouin function B_J, the isothermal normalized magnetization can be derived as a unique function of g and J.[27] In this study, we have kept g = 2, and the experimental isothermal magnetization curves observed between 4 and 300 K are fitted with the Brillouin functions. The best fitted B_J yields the J value for the experimental curves at various temperatures. Figure 4 shows J

DOI: 10.1021/acs.jpcc.5b02284
J. Phys. Chem. C 2015, 119, 12698−12702

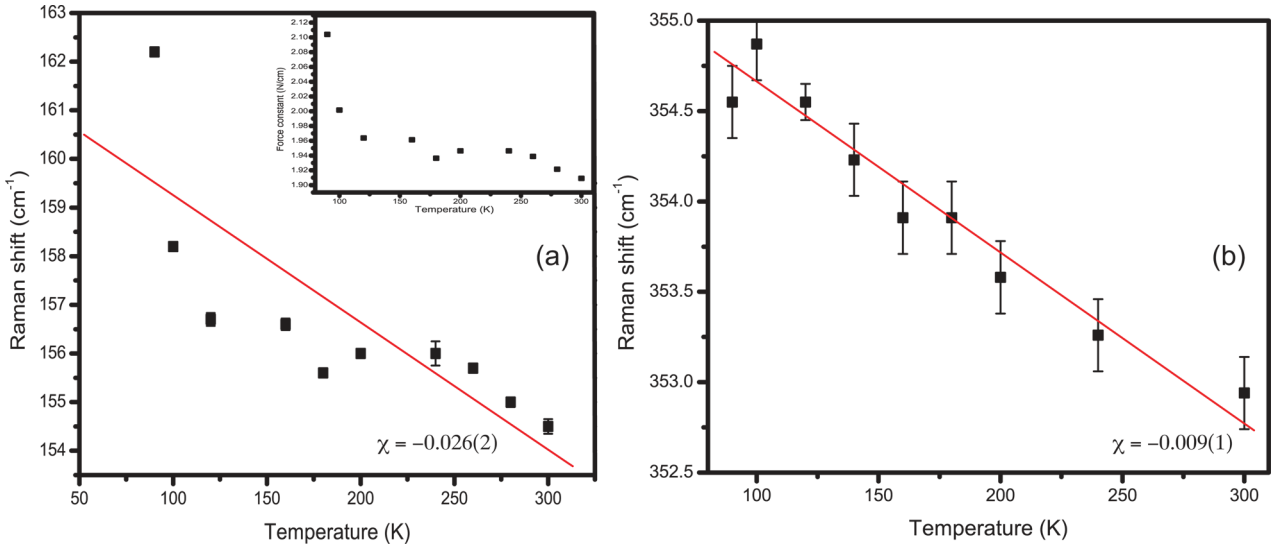

Figure 3. Temperature-dependent Raman shifts observed at (a) 155 cm^{-1} and (b) 352 cm^{-1} due to Gd−C and C−C vibrational modes, respectively. The inset of (a) shows the force constant variation with temperature for Gd−C_{82} interaction.

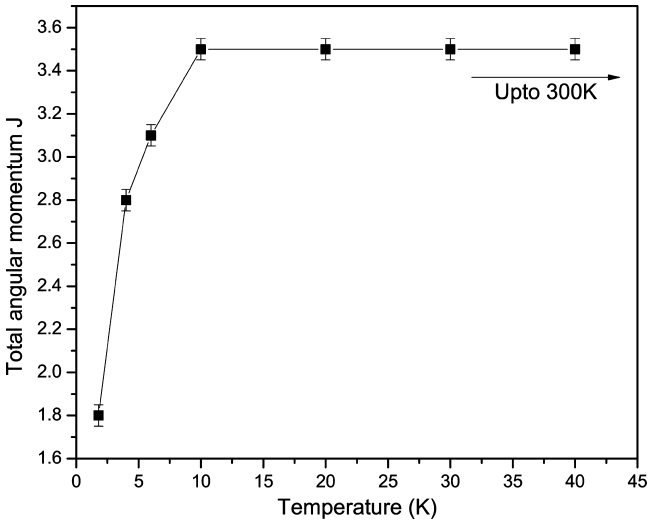

Figure 4. Dependence of total angular momentum J with temperature in Gd@C_{82} between 4 and 300 K.

versus temperature for Gd@C_{82} in the range 4−300 K. It is evident from the figure that J is constant (≈3.5) above 15 K, revealing that no change in the oxidation state of the ion occurs above 15 K. This is why we conclude that the observed blueshifts in the Raman spectrum at 90 K are not due to the variation in the oxidation states of the metal ion; rather, it could be due to external perturbations such as mechanical stress, strain, and thermal effects.

The net displacement of the atoms changes the frequencies of vibration resulting in a shifted Raman peak. A compressive stress leads to a blueshift, wheres tensile stress redshifts the Raman frequencies.[28−30] In addition to the stress and/or strain, the Raman frequencies also depend on the sample temperature. The higher-order terms in the crystal potential lead to explicit anharmonic interactions of phonons at constant volume, whereas thermal expansion in the solid changes the volume and effective bond strength. The collective thermal response in solid modifies the Raman frequencies and line widths with temperature. As we have measured the Raman spectra at constant pressure instead of constant volume, both thermal expansion and anharmonic contributions might be present in the Raman shifts with temperature.

A general temperature behavior of the Raman frequencies (ω) can be defined as[10,11]

$$\omega(T) = \omega_0 + \chi T \tag{2}$$

where ω_0 is the frequency at absolute zero and χ is the first-order temperature coefficient containing thermal expansion and anharmonic contribution to the energy shifts. As our experimental temperature range 90−300 K is significantly below the graphite Debye temperature, the anharmonic contribution is expected to be small.[11] The experimental data are fitted by the above equation, and the responses of ω at 155 and 352 cm^{-1} are evaluated. The temperature coefficients χ of 155 and 352 cm^{-1} peaks are found to be −0.026(7) and −0.009(1) cm^{-1}/K. High bending strain energy is often observed in carbon nanotube rings and fullerenes which makes the softening of the C−C bond more difficult.[31−33] This is why the C−C bond strength and its corresponding temperature coefficient in Gd@C_{82} has less dependence on temperature as compared to that seen in graphene and straight nanotubes.[10,31] Being more sensitive to the crystal field effects, the metal−cage vibrations show higher temperature coefficients than the C−C cage modes.

The extrapolated frequencies ω_0 for 155 and 352 cm^{-1} peaks are observed to be 162(1) and 355.6(2) cm^{-1}, respectively. The observed blueshifts in both metal−cage and cage internal modes of vibration can be caused by the thermal contraction of the cage at low temperatures which in turn modifies the Gd−C and C−C bond length and their strength of interaction. The X-ray absorption analysis performed on Gd@C_{82} by Giefers et al. has also illustrated a weak temperature dependence of Gd−C distance. The change in the metal−ion distance with temperature is attributed to the effects of thermal vibrations and distortion in the local environment of the Gd ion near carbon hexagons at low temperatures.[24]

The observed temperature coefficients for Gd−C and C−C modes in Gd@C_{82} are found to be comparable to those reported for various other carbon nanomaterials including graphene and carbon nanotubes (CNTs).[10−13,34−36] In

DOI: 10.1021/acs.jpcc.5b02284
J. Phys. Chem. C 2015, 119, 12698−12702

graphene, the temperature coefficients corresponding to a graphitic band are found to be −0.016 and −0.015 cm^{-1}/K for mono- and bilayered sheets,[10] whereas in CNT rings, the temperature coefficients of radial breathing modes are found to be varying between −0.0057 and −0.0263 cm^{-1}/K. These temperature coefficients are found to be shape dependent and also explain the thermal stability of nanotube rings over linear tubes.[31] In both graphene and CNTs, the thermal contraction is reportedly an effect of anharmonic lattice potential which affects the thermal stability and thus the thermal conductivity of these nanomaterials.[10,11,31]

Figure 5 shows the temperature-dependent full width at half maxima (fwhm) of the 155 cm^{-1} peak as a function of

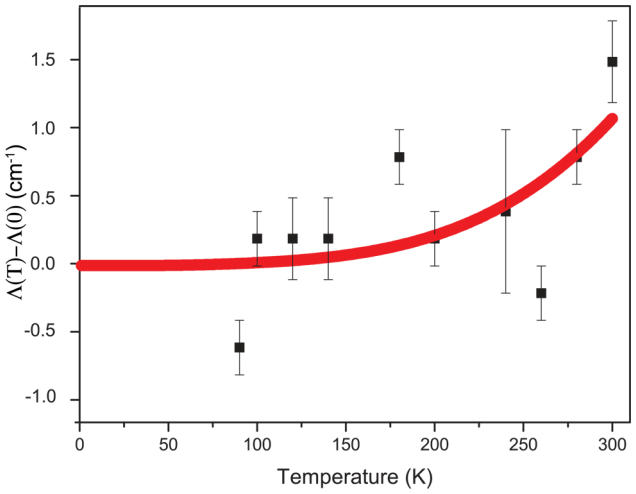

Figure 5. Line width difference $\Lambda(T) - \Lambda(0)$ between temperature T and 0 K of the 155 cm^{-1} peak plotted against temperature T.

temperature. The temperature-dependent line widths $\Lambda(T)$ can be governed by the phonon occupation given by the Boltzmann distribution at the Raman frequency ω[36−38]

$$\Lambda(T) - \Lambda(0) = \left[\frac{A}{\exp\left(\frac{\hbar\omega_0}{k_B T}\right) - 1} + \frac{B}{\left(\exp\left(\frac{\hbar\omega_0}{k_B T}\right) - 1\right)^3} \right] \quad (3)$$

where $\Lambda(0)$ is temperature-independent fwhm and A and B are the peak broadening components due to higher-order anharmonicities. The observed line width difference $\Lambda(T) - \Lambda(0)$ as a function of temperature is fitted with the above equation and is shown in Figure 5. At higher temperatures, the fwhm increases linearly with temperature, whereas at low temperatures and when extrapolated to absolute zero ($T \rightarrow 0$ K), it converges to about 2.5(2) cm^{-1} ($\Lambda(0)$). It is only above 200 K that the anharmonic effects in peak broadening are evident. A and B are evaluated as 0.17 (4) and 1.5(7) cm^{-1}, respectively, revealing the presence of small anharmonic effects in the peak broadening. The reduced line width could be associated with the freezing of cage at low temperatures which in turn strengthens the interaction between the Gd ion and the cage and also reduces the anharmonic phonon decay.[39]

CONCLUSION

In summary, we reported the first experimental investigation of temperature-dependent Raman spectra for $Gd@C_{82}$ thin films. Two Raman frequencies observed at 155 and 352 cm^{-1} at 300 K are attributed to metal−cage and internal cage vibrational modes, respectively. At 90 K, a blueshift in both frequencies is observed which is demonstrated by the thermal and anharmonic effects in the fullerene cage. The line width of the 155 cm^{-1} peak reduces with temperature and converges to 2.5 cm^{-1} at absolute zero. Although thermal effects play a significant role in the metal−cage bond strength (k), no change in the oxidation state of the Gd ion is observed above 15 K. The extracted temperature coefficient of the 155 cm^{-1} peak is χ = −0.026(7), whereas for the 352 cm^{-1} peak it is χ = −0.009(1) cm^{-1}/K which are at par with those reported for other carbon nanomaterials. Our results consider both the pure-temperature as well as pure-volume effects in the evaluated temperature coefficients where the blueshift in the metal−cage vibrational frequency is attributed to thermal contraction of the cage, whereas the decrease in line width at lower temperatures occurs due to reduced anharmonic effects. With the help of these temperature coefficients, a Raman spectrometer can now be treated as a noncontact thermometer for observing the temperature of $Gd@C_{82}$.

AUTHOR INFORMATION

Corresponding Author

*Phone: +91 3592 232080. E-mail: archana.tiwari.ox@gmail.com.

Notes

The authors declare no competing financial interest.

ACKNOWLEDGMENTS

This work is supported by UGC-DAE-CSR Indore.

REFERENCES

(1) Shinohara, H. Endohedral Metallofullerenes. *Rep. Prog. Phys.* **2000**, *63*, 843−892.
(2) Popov, A. A.; Yang, S.; Dunsch, L. Endohedral Fullerenes. *Chem. Rev.* **2013**, *113*, 5989−6113.
(3) Lu, X.; Feng, L.; Akasaka, T.; Nagase, S. Current Status and Future Developments of Endohedral Metallofullerenes. *Chem. Soc. Rev.* **2012**, *41*, 7723−7760.
(4) Nishibori, E.; Iwata, K.; Sakata, M. Anomalous Endohedral Structure of $Gd@C_{82}$ Metallofullerenes. *Phys. Rev. B* **2004**, *69*, 113412.
(5) Akasaka, T.; Nagase, S.; Kobayashi, K.; Wälchli, M.; Yamamoto, K.; Funasaka, H.; Kako, M.; Hoshino, T.; Erata, T. ^{13}C and ^{139}La NMR Studies of $La_2@C_{80}$: First Evidence for Circular Motion of Metal Atoms in Endohedral Dimetallofullerenes. *Angew. Chem., Int. Ed. Engl.* **1997**, *36*, 1643−1645.
(6) Lebedkin, S.; Renker, B.; Heid, R.; Schober, H.; Rietschel, H. A Spectroscopic Study of $M@C_{82}$ Metallofullerenes: Raman, Far-Infrared, and Neutron Scattering Results. *Appl. Phys. A: Mater. Sci. Process.* **1998**, *66*, 273−280.
(7) Krause, M.; Kuran, P.; Kirbach, U.; Dunsch, L. Raman and Infrared Spectra of $Tm@C_{82}$ and $Gd@C_{82}$. *Carbon* **1999**, *37*, 113−115.
(8) Krause, M.; Hulman, M.; Kuzmany, H.; Dubay, O.; Kresse, G.; Vietze, K.; Seifert, G.; Wang, C.; Shinohara, H. Fullerene Quantum Gyroscope. *Phys. Rev. Lett.* **2004**, *93*, 137403.
(9) Krishnan, R. Temperature Variations of the Raman Frequencies in Diamond. *Proc. Indian Acad. Sci., Sect. A* **1946**, 45−57.
(10) Calizo, I.; Balandin, A. A.; Bao, W.; Miao, F.; Lau, C. N. Temperature Dependence of the Raman Spectra of Graphene and Graphene Multilayers. *Nano Lett.* **2007**, *7*, 2645−2649.
(11) Ci, L.; Zhou, Z.; Song, L.; Yan, X.; Liu, D.; Yuan, H.; Gao, Y.; Wang, J.; Liu, L.; Zhou, W.; et al. Temperature Dependence of

DOI: 10.1021/acs.jpcc.5b02284
J. Phys. Chem. C 2015, 119, 12698−12702

Resonant Raman Scattering in Double-Wall Carbon Nanotubes. *Appl. Phys. Lett.* **2003**, *82*, 3098−3100.
(12) Tan, P. H.; Deng, Y.; Zhao, Q.; Cheng, W. The Intrinsic Temperature Effect of the Raman Spectra of Graphite. *Appl. Phys. Lett.* **1999**, *74*, 1818−1820.
(13) Raravikar, N. R.; Keblinski, P.; Rao, A. M.; Dresselhaus, M. S.; Schadler, L. S.; Ajayan, P. M. Temperature Dependence of Radial Breathing Mode Raman Frequency of Single-Walled Carbon Nanotubes. *Phys. Rev. B* **2002**, *66*, 235424.
(14) Chase, B.; Herron, N.; Holler, E. Vibrational Spectroscopy of Fullerenes (C_{60} and C_{70}). Temperature Dependant Studies. *J. Phys. Chem.* **1992**, *96*, 4262−4266.
(15) Krause, M.; Hulman, M.; Kuzmany, H.; Dennis, T. J. S.; Inakuma, M.; S, H. Diatomic Metal Encapsulates in Fullerene Cages: A Raman and Infrared Analysis of C_{84} and $Sc_2@C_{84}$ with D_{2d} Symmetry. *J. Chem. Phys.* **1999**, *111*, 7976−7984.
(16) Kuzmany, H.; Pfeiffer, R.; Hulman, M.; Kramberger, C. Raman Spectroscopy of Fullerenes and Fullerene-Nanotube Composites. *Philos. Trans. R. Soc. London, Ser. A: Math., Phys. Eng. Sci.* **2004**, *362*, 2375−2406.
(17) Nakai, H.; Ebihara, T.; Tsutsui, S.; Mizumaki, M.; Kawamura, N.; Michimura, S.; Inami, T.; Nakamura, T.; Kondo, A.; Kindo, K.; et al. Temperature and Magnetic Field Dependent Yb Valence in $YbRh_2Si_2$ Observed by X-Ray Absorption Spectroscopy. *J. Phys. Soc. Jpn.* **2013**, *82*, 124712.
(18) Svitlyk, V.; Hermes, W.; Chevalier, B.; Matar, S. F.; Gaudin, E.; Voßwinkel, D.; Chernyshov, D.; Hoffmann, R.-D.; Pöttgen, R. Change of the Cerium Valence with Temperature-Structure and Chemical Bonding of HT-CeRhGe. *Solid State Sci.* **2013**, *21*, 6−10.
(19) Zhang, Y.; Popov, A. A.; Dunsch, L. Endohedral Metal or a Fullerene Cage Based Oxidation? Redox Duality of Nitride Clusterfullerenes $Ce_xM_{3-x}N@C_{78-88}$ (x= 1, 2; M= Sc and Y) Dictated by the Encaged Metals and the Carbon Cage Size. *Nanoscale* **2014**, *6*, 1038−1048.
(20) Sueki, K.; Akiyama, K.; Kikuchi, K.; Nakahara, H. A C_{82} Carbon Cage Stable toward Two Different Oxidation States of Endohedral Metal Atoms. *J. Phys. Chem. B* **1999**, *103*, 1390−1392.
(21) Wagberg, T.; Launois, P.; Moret, R.; Huang, H.; Yang, S.; Li, I.; Tang, Z. Study by X-Ray Diffraction and Raman Spectroscopy of a $Dy@C_{82}$ Single Crystal. *Eur. Phys. J. B* **2003**, *35*, 371−375.
(22) Burke, B. G.; Chan, J.; Williams, K. A.; Ge, J.; Shu, C.; Fu, W.; Dorn, H. C.; Kushmerick, J. G.; Puretzky, A. A.; Geohegan, D. B. Investigation of $Gd_3N@C_{2n}$ ($40 < n < 44$) Family by Raman and Inelastic Electron Tunneling Spectroscopy. *Phys. Rev. B* **2010**, *81*, 115423.
(23) Huang, H. J.; Yang, S. H.; Zhang, X. X. Magnetic Properties of Heavy Rare-Earth Metallofullerenes $M@C_{82}$ (M =Gd, Tb, Dy, Ho, and Er). *J. Phys. Chem. B* **2000**, *104*, 1473−1482.
(24) Giefers, H.; Nessel, F.; Gyosry, S.; Strecker, M.; Wortmanna, G.; Grushko, Y.; Alekseev, E.; Kozlov, V. Gd-LIII EXAFS Study of Structural and Dynamic Properties of $Gd@C_{82}$ Between 10 and 300 K. *Carbon* **1999**, *37*, 721−725.
(25) Huang, H.; Yang, S.; Zhang, X. Magnetic Behavior of Pure Endohedral Metallofullerene $Ho@C_{82}$: A Comparison with $Gd@C_{82}$. *J. Phys. Chem. B* **1999**, *103*, 5928−5932.
(26) Senapati, L.; Schrier, J.; Whaley, K. B. Electronic Transport, Structure, and Energetics of Endohedral Gd@ C_{82} Metallofullerenes. *Nano Lett.* **2004**, *4*, 2073−2078.
(27) Blundell, S. *Magnetism in Condensed Matter*; Oxford University Press: Oxford, U.K., 2001.
(28) Rau, U., Abou-Ras, D.; Kirchartz, T. *Advanced Characterization Techniques for Thin Film Solar Cells*; John Wiley & Sons: Weinheim, Germany, 2011.
(29) Xu, C.; Zhang, P.; Yan, L. Blue Shift of Raman Peak from Coated TiO_2 Nanoparticles. *J. Raman Spectrosc.* **2001**, *32*, 862−865.
(30) Ni, Z.; Chen, W.; Fan, X.; Kuo, J.; Yu, T.; Wee, A.; Shen, Z. Raman Spectroscopy of Epitaxial Graphene on a SiC Substrate. *Phys. Rev. B* **2008**, *77*, 115416.
(31) Song, L.; Ma, W.; Ren, Y.; Zhou, W.; Xie, S.; Tan, P.; Sun, L. Temperature Dependence of Raman Spectra in Single-Walled Carbon Nanotube Rings. *Appl. Phys. Lett.* **2008**, *92*, 121905.
(32) Robertson, D.; Brenner, D.; Mintmire, J. Energetics of Nanoscale Graphitic Tubules. *Phys. Rev. B* **1992**, *45*, 12592.
(33) Handschuh, H.; Ganteför, G.; Kessler, B.; Bechthold, P. S.; Eberhardt, W. Stable Configurations of Carbon Clusters: Chains, Rings, and Fullerenes. *Phys. Rev. Lett.* **1995**, *74*, 1095−1098.
(34) Zhang, Q.; Yang, D.; Wang, S.; Yoon, S.; Ahn, J. Influences of Temperature on the Raman Spectra of Single-Walled Carbon Nanotubes. *Smart Mater. Struct.* **2006**, *15*, S1−S4.
(35) Zhang, Y.; Xie, L.; Zhang, J.; Wu, Z.; Liu, Z. Temperature Coefficients of Raman Frequency of Individual Single-Walled Carbon Nanotubes. *J. Phys. Chem. C* **2007**, *111*, 14031−14034.
(36) Chatzakis, I.; Yan, H.; Song, D.; Berciaud, S.; Heinz, T. F. Temperature Dependence of the Anharmonic Decay of Optical Phonons in Carbon Nanotubes and Graphite. *Phys. Rev. B* **2011**, *83*, 205411.
(37) Giura, P.; Bonini, N.; Creff, G.; Brubach, J.; Roy, P.; Lazzeri, M. Temperature Evolution of Infrared-and Raman-Active Phonons in Graphite. *Phys. Rev. B* **2012**, *86*, 121404.
(38) Fugallo, G.; Cepellotti, A.; Paulatto, L.; Lazzeri, M.; Marzari, N.; Mauri, F. Thermal Conductivity of Graphene and Graphite: Collective Excitations and Mean Free Paths. *Nano Lett.* **2014**, *14*, 6109−6114.
(39) Chen, Y.; Peng, B.; Wang, B. Raman Spectra and Temperature-Dependent Raman Scattering of Silicon Nanowires. *J. Phys. Chem. C* **2007**, *111*, 5855−5858.

DOI: 10.1021/acs.jpcc.5b02284
J. Phys. Chem. C 2015, 119, 12698−12702